Progress In Electromagnetics Research, Vol. 113, 17–46, 2011

JOINT AZIMUTH-ELEVATION/(-RANGE) ESTIMATION OF MIXED NEAR-FIELD AND FAR-FIELD SOURCES USING TWO-STAGE SEPARATED STEERING VECTOR-BASED ALGORITHM

J. Liang and D. Liu

School of Automation & Information Engineering
Xi'an University of Technology, Xi'an, China

X. Zeng

College of Management
Shenzhen University, China

W. Wang

Tianjin Key Laboratory for Advanced Signal Processing
Civil Aviation University of China, China

J. Zhang

School of Computer Science and Engineering
Xi'an University of Technology, Xi'an, China

H. Chen

Graduate School of Information Science and Technology
University of Tokyo, Japan

Abstract—Passive source localization has wide applications in array signal processing. In the practical applications, the observations collected by an array may be "arbitrary"-field signals, i.e., which are either mixed near-field and far-field signals or multiple near-field signals or multiple far-field signals. With a cross array, a two-stage separated steering vector-based algorithm is developed to localize "arbitrary"-field narrowband sources in the spherical coordinates. The key points of this paper are: i) different physical steering vectors of near-field

Received 1 November 2010, Accepted 23 December 2010, Scheduled 25 January 2011
Corresponding author: Junli Liang (liangjunli@xaut.edu.cn).

and far-field sources are transformed into the virtual ones with the same form, thus linearizing the quadratic phases of near-field sources and allowing the same operations for near-field and far-field sources; ii) the virtual steering vector is separated into two parts and restored by introducing a special phase angle, and thus it is used to estimate the azimuth-elevation arrival-angles of "arbitrary"-field sources; and iii) special Hermitian matrices are constructed using the separated physical steering vector and their eigenvalue decomposition (EVD) are performed, thus the ranges of near-field sources are easily obtained from the eigenvector being corresponding to the smallest eigenvalue. The proposed algorithm can localize "arbitrary"-field sources without pairing parameters and multidimensional search. Simulation results are provided to validate the performance of the proposed method.

1. INTRODUCTION

Passive source localization is a key problem of array signal processing involved in radar, sonar, electronic surveillance, and seismic exploration applications [1]. The waves emitted by far-field sources [2, 3] can be considered as plane ones at the sensor array [4–10]. However, for near-field (*Fresnel* region) sources, the wavefronts are no longer planar [2, 3]. Unlike far-field sources, near field sources introduce quadratic phases, which are functions of both azimuth angle and range [11–21]. Therefore, the existing far-field source localization algorithms [4–10] cannot be utilized.

1.1. Related Work

Many localization methods for near-field sources [11–24] have already been developed, including the Wigner-Ville distribution-based method [11], the maximum likelihood method [12], the linear prediction methods [13–15], the two-dimensional (2-D) MUSIC methods [16–19], and the ESPRIT-like methods [20, 21]. However, all these methods are limited to localize near-field sources only in azimuth angle and range.

Recently, some algorithms [25–29] are presented to localize near-field sources in the spherical coordinates (i.e., joint azimuth-elevation-range estimation problem). The expectation-maximization (EM) algorithm based on the maximum likelihood criterion is proposed in [25], but it requires search computation and iteration process and cannot give the estimations with closed analytic solution. In [26], Challa and Shamsunder developed a Unitary ESPRIT algorithm, in which an additional parameter pairing procedure is required. The method in [27] depends heavily on different carrier

frequencies, approximated sinusoidal signals, and extremely high sampling narrowband data. The spectral search-based method in [28] is applied to localize near-field sources only in underwater environment by exploiting the characteristics of vector hydrophones [28]. Although it is of low computational complexity, the second-order statistics-based algorithm in [29] suffers heavy aperture loss and requires a complicated quadratic phase transformation method [30] to pair the separately estimated parameters.

1.2. Main Difficulties in Localizing "Arbitrary"-field Sources

In the practical applications, the observations collected by an array may be "arbitrary"-field signals [31–39], i.e., which are either mixed near-field and far-field signals or multiple near-field signals, or multiple far-field signals, as in passive target localizations in radar, sonar, and electronic surveillance. Therefore, it is necessary to develop an algorithm with the flexibility to localize "arbitrary"-field sources.

There are two different signal models for near-field and far-field sources due to their different phase forms. Can the near-field source localization algorithms be applied to far-field case? When more than one far-field source exists, the virtual steering matrix defined in Eq. (13) of [29] no longer has full column rank and thus the second-order statistics-based algorithm will break down. Although the Unitary ESPRIT algorithm developed for near-field source localization can be applied to localize "arbitrary"-field sources (elaborated in Part IV), it requires pairing parameters and suffers array aperture loss since it deals with the two subarrays of a cross array separately. It seems that the extended three-dimensional MUSIC algorithm [4] can localize "arbitrary"-field sources without any matching operation or array aperture loss. However, it suffers from the heavy computational load due to search computation as that of the EM algorithm [25]. Can the far-field source localization algorithms be applied to near-field case? Since the far-field signal model does not incorporate the range information, the far-field source localization algorithms does not suit near-field situation, such as the ESPRIT algorithm [6] for azimuth-elevation arrival-angles estimation.

Based on the aforementioned discussion, the main difficulties of passive source localization consist in: i) alleviating heavy aperture loss; ii) eliminating the matching operation; iii) avoiding multidimensional search; and iv) localizing "arbitrary"-field sources.

1.3. Key Points and Contributions

In contrast to the two-stage MUSIC method in [39], where the sensor array and sources are in the same plane (i.e., jointly estimating azimuth angles and ranges for near-field sources, and azimuth angles for far-field sources), the proposed algorithm pays attention to localizing "arbitrary"-field sources in the spherical coordinates [25–29], i.e., jointly estimating azimuth-elevation arrival-angles and ranges for near-field sources, and azimuth-elevation arrival-angles for far-field sources.

The key points and contributions of this paper are summarized as follows:

Constructing a special cumulant matrix: Similar to [26, 29], a cross-array is discussed in this paper, which is often adopted in microphone array configuration. Near-field and far-field sources have different signal models. The intuition then is to explore two methods respectively for the two types of sources. Obviously it is difficult to apply two methods to the same array observations for localizing "arbitrary"-field sources. In order to develop a flexible algorithm to localize "arbitrary"-field sources, we derive a special cumulant matrix that is the product of three components. In the first component, virtual steering matrix, the quadratic phase terms of near-field sources are canceled by exploiting the multiple degrees of freedom available from cumulants [40–44] whereas the linear phase characteristic inherent is retained for far-field sources. Therefore, near-field and far-field sources share the common phase form in the virtual steering matrix, allowing efficient processing via the same computations. The third component, containing the range information of near-field sources, is just the physical steering matrix of the actual sensor array. Moreover, from the left and right singular-vectors of the cumulant matrix, two respective orthogonal bases for the range space of the virtual steering matrix and the null space of the physical steering matrix can be simultaneously obtained to facilitate the preceding two-stage separated steering vector-based algorithm.

Restoring the virtual steering vector: Since the virtual steering vectors of "arbitrary"-field sources possess linear phase property, it is possible to obtain their azimuth-elevation arrival-angles from the vectors. In Part III, we develop a new approach to restore the virtual steering vector from the cumulant matrix. We separate the virtual steering vector into two parts by introducing a new phase angle, where the first part is the functional matrix of the introduced phase angle whereas the second part is the functional vector of other parameters. The general ESPRIT algorithm [45] is applied to the transformed subarrays for estimating the introduced phase angle. With the estimated phase angle, the second part of the separated steering

vector is restored using the eigenvalue decomposition (EVD) of some particular Hermitian matrices. By combining the first and second parts, the virtual steering vector is recovered and the azimuth-elevation arrival-angles of "arbitrary"- field sources can be easily obtained.

We stress that unlike the general ESPRIT algorithms of [28, 45], the presented approach does not require the subarrays have general rotational invariance geometry, but transforms two orthogonal subarrays (in the virtual steering vector of the cumulant matrix) of the cross array to two new ones with general rotational invariance geometry (with respect to the introduced phase angle). In addition, it pays attention to separating and restoring the virtual steering vector so as to estimate azimuth-elevation arrival-angles from the restored one [28, 45]. Therefore, it can be considered as the extension from one-dimensional arrival-angle estimation algorithm [45] to two-dimensional one. Moreover, unlike [28], it has wider applications since it uses omni-directional sensors instead of the vector hydrophone only in underwater environment.

Estimating ranges of near-field sources by separating the physical steering vector: Using two intermediate parameters we separate the physical steering vector into two parts, the functional matrix of these two parameters and the vector containing the range information of near-field sources. The combinations of the first part and the right singular-vectors of the cumulant matrix yield a special Hermitian matrix. From its eigenvector corresponding to the smallest eigenvalue, we can restore the second part of the separated physical steering vector and obtain the ranges of near-field sources.

Notation is as follows. Vectors and matrices are referred to as lowercase and uppercase bold letters, respectively. The transpose matrix is denoted by superscript $(\bullet)^T$, the conjugate transpose by superscript $(\bullet)^H$, and the conjugate by superscript $(\bullet)^*$. $\mathrm{diag}\{\bullet, \ldots, \bullet\}$ stands for a square diagonal matrix ($\searrow$, going from the upper left corner to the lower right corner of the main diagonal), andadiag$\{\bullet, \ldots, \bullet\}$ represents a square anti-diagonal matrix($\nearrow$, going from the lower left corner to the upper right corner of the main diagonal).

The rest of this paper is organized as follows. The signal model is introduced in Section 2. A two-stage separated steering vector-based algorithm is developed in Section 3. Simulation results are presented in Section 4. Conclusions are drawn in Section 5.

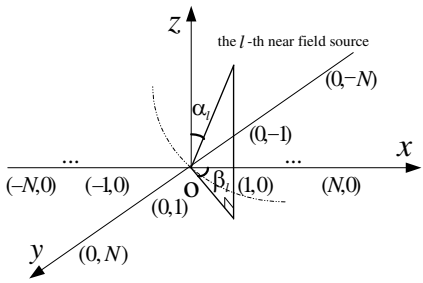

Figure 1. Centro-symmetric cross array configuration.

2. "ARBITRARY"-FIELD SIGNAL MODEL

Consider L (near-field† or far-field) narrowband, independent radiating sources impinging upon a centro-symmetric cross-array aligned with the x and y axes, as shown in Fig. 1. The cross one is chosen as the phase reference point. Subarray in each axis consists of $2N+1$ omni-directional sensors with uniform element spacing d. The sampled signals collected by the $(j,0)$th and $(0,m)$th sensors can be respectively expressed as [1–3]:

$$x_{j,0}(k) = \sum_{l=1}^{L} s_l(k) e^{i\tau_{xl}(j)} + n_{j,0}(k), \qquad i = \sqrt{-1}\,; \quad j = -N, \ldots, -1, 0, 1, \ldots, N, \tag{1}$$

and

$$x_{0,m}(k) = \sum_{l=1}^{L} s_l(k) e^{i\tau_{yl}(m)} + n_{0,m}(k), \quad m = -N, \ldots, -1, 1, \ldots, N, \tag{2}$$

where $s_l(k)$ denotes the lth narrowband source signal at time k, and $\{n_{j,0}(k), n_{0,m}(k)\}$ represents the additive Gaussian noise. In addition, $\tau_{xl}(j)$ is the propagation delay associated with the lth source between the $(0,0)$th and $(j,0)$th sensors; while $\tau_{yl}(m)$ is the propagation delay associated with the lth source between the $(0,0)$th and $(0,m)$th sensors. If the lth source lies in the near field, the signal phases $\tau_{xl}(j)$ and $\tau_{yl}(m)$ are parameterized in terms of the intermediate parameters $(\gamma_{xl}, \phi_{xl}, \gamma_{yl}, \phi_{yl})$, and have the following forms‡ respectively:

$$\tau_{xl}(j) = j\gamma_{xl} + j^2\phi_{xl}, \tag{3}$$

† Note that Fresnel zone (i.e., near-field) lies in the radiating zone $[\lambda/(2\pi), 2D^2/\lambda]$, where D is the array dimension (see [2, 3] for details). However, the radiating zone in the far-field case is one beyond $[0, 2D^2/\lambda]$.

‡ The second-order Taylor series approximation is found in many references on near-field source localization [3, 11–15, 19–29]. The effect of this approximation on the estimation

and

$$\tau_{yl}(m) = m\gamma_{yl} + m^2\phi_{yl}. \tag{4}$$

In this case, ϕ_{xl} and ϕ_{yl} cannot be neglected. In turn $(\gamma_{xl}, \phi_{xl}, \gamma_{yl}, \phi_{yl})$ are functions of the lth source's elevation angle α_l, azimuth angle β_l, and range r_l, and have the following forms respectively:

$$\gamma_{xl} = -\frac{2\pi d \sin\alpha_l \cos\beta_l}{\lambda}, \tag{5}$$

$$\phi_{xl} = \frac{\pi d^2 \left(1 - \sin^2\alpha_l \cos^2\beta_l\right)}{\lambda r_l}, \tag{6}$$

$$\gamma_{yl} = -\frac{2\pi d \sin\alpha_l \sin\beta_l}{\lambda}, \tag{7}$$

and

$$\phi_{yl} = \frac{\pi d^2 \left(1 - \sin^2\alpha_l \sin^2\beta_l\right)}{\lambda r_l}. \tag{8}$$

From Eqs. (5)–(8), we can see that the parameters (α_l, β_l, r_l) can be obtained by firstly estimating the intermediate parameters $(\gamma_{xl}, \phi_{xl}, \gamma_{yl}, \phi_{yl})$ and then solving Eqs. (5)–(8).

Otherwise, if the lth source lies in the far field, $\tau_{xl}(j)$ and $\tau_{yl}(m)$ have the following forms respectively [2–10]:

$$\tau_{xl}(j) = j\gamma_{xl}, \tag{9}$$

and

$$\tau_{yl}(m) = m\gamma_{yl}. \tag{10}$$

In Eqs. (9) and (10), both ϕ_{xl} and ϕ_{yl} are approximated as zero due to farther ranges of far-field sources [2, 3]. Therefore, far-field sources can be considered as a special case of near-field sources, where $\phi_{xl} = 0$ and $\phi_{yl} = 0$.

In a matrix form, the sensor output can be written as

$$\mathbf{x}(k) = \mathbf{A}\mathbf{s}(k) + \mathbf{n}(k), \quad k = 0, \ldots, K-1, \tag{11}$$

where

$$\begin{aligned}\mathbf{n}(k) = [&n_{-N,0}(k)\ n_{-N+1,0}(k)\ \ldots\ n_{-1,0}(k)\\ &n_{1,0}(k)\ \ldots\ n_{N-1,0}(k)\ n_{N,0}(k)\ n_{0,0}(k)\\ &n_{0,-N}(k)\ n_{0,-N+1}(k)\ \ldots\ n_{0,-1}(k)\\ &n_{0,1}(k)\ \ldots\ n_{0,N-1}(k)\ n_{0,N}(k)]^T\end{aligned} \tag{12}$$

performance is elaborated in [11], where it was shown that for range greater than ten times the array length, the error introduced is less than 0.5%.

$$\mathbf{s}(k) = [s_1(k)\ s_2(k)\dots s_L(k)]^T, \tag{13}$$

$$\begin{aligned}\mathbf{x}(k) = [&x_{-N,0}(k)\ x_{-N+1,0}(k)\ \dots\ x_{-1,0}(k)\\ &x_{1,0}(k)\ \dots\ x_{N-1,0}(k)\ x_{N,0}(k)\ x_{0,0}(k)\\ &x_{0,-N}(k)\ x_{0,-N+1}(k)\ \dots\ x_{0,-1}(k)\\ &x_{0,1}(k)\ \dots\ x_{0,N-1}(k)\ x_{0,N}(k)]^T\end{aligned} \tag{14}$$

and the $(4N+1)\times L$-dimensional physical steering matrix

$$\mathbf{A} = [\mathbf{a}(\gamma_{x1},\phi_{x1},\gamma_{y1},\phi_{y1})\,\mathbf{a}(\gamma_{x2},\phi_{x2},\gamma_{y2},\phi_{y2})\ \dots\ \mathbf{a}(\gamma_{xL},\phi_{xL},\gamma_{yL},\phi_{yL})] \tag{15}$$

Note that the form of the steering vector $\mathbf{a}(\gamma_{xl},\phi_{xl},\gamma_{yl},\phi_{yl})$ in (15) depends on whether the lth source is in the far field or near field. If this source is in the near field, $\mathbf{a}(\gamma_{xl},\phi_{xl},\gamma_{yl},\phi_{yl})$ has the following quadratic phase form:

$$\begin{aligned}&\mathbf{a}(\gamma_{xl},\phi_{xl},\gamma_{yl},\phi_{yl})\\ =\ &\Big[e^{i[(-N)\gamma_{xl}+(-N)^2\phi_{xl}]}\ e^{i[(-N+1)\gamma_{xl}+(-N+1)^2\phi_{xl}]}\ \dots\ e^{i[-\gamma_{xl}+\phi_{xl}]}\\ &e^{i[\gamma_{xl}+\phi_{xl}]}\ \dots e^{i[(N-1)\gamma_{xl}+(N-1)^2\phi_{xl}]}\ e^{i[N\gamma_{xl}+N^2\phi_{xl}]}\ 1\\ &e^{i[(-N)\gamma_{yl}+(-N)^2\phi_{yl}]}\ e^{i[(-N+1)\gamma_{yl}+(-N+1)^2\phi_{yl}]}\ \dots e^{i[-\gamma_{yl}+\phi_{yl}]}\\ &e^{i[\gamma_{yl}+\phi_{yl}]}\ \dots\ e^{i[(N-1)\gamma_{yl}+(N-1)^2\phi_{yl}]}\ e^{i[N\gamma_{yl}+N^2\phi_{yl}]}\Big]^T\end{aligned} \tag{16}$$

Otherwise, if the lth source is in the far field, $\mathbf{a}(\gamma_{xl},\phi_{xl},\gamma_{yl},\phi_{yl})$ has the following linear phase form due to $\phi_{xl}=0$ and $\phi_{yl}=0$ [2–10]:

$$\begin{aligned}&\mathbf{a}(\gamma_{xl},\phi_{xl},\gamma_{yl},\phi_{yl})\\ =&\Big[e^{i[(-N)\gamma_{xl}]}\ e^{i[(-N+1)\gamma_{xl}]}\ \dots\ e^{i[-\gamma_{xl}]}\ \ e^{i[\gamma_{xl}]}\ \dots e^{i[(N-1)\gamma_{xl}]}\ e^{i[N\gamma_{xl}]}\ 1\\ &e^{i[(-N)\gamma_{yl}]}\ e^{i[(-N+1)\gamma_{yl}]}\ \dots e^{i[-\gamma_{yl}]}\ \ e^{i[\gamma_{yl}]}\ \dots\ e^{i[(N-1)\gamma_{yl}]}\ e^{i[N\gamma_{yl}]}\Big]^T.\end{aligned} \tag{17}$$

The objective of our algorithm is to jointly estimate the 3-D parameters (α_l,β_l,r_l) for near-field sources and the 2-D parameters (α_l,β_l) for far-field sources, given the array data $\mathbf{x}(k)$ for $k=0,\dots,K-1$.

Throughout the rest of the article, these hypotheses are assumed to hold:

1) The source signals are statistically mutually independent, narrowband stationary processes with nonzero kurtosis;
2) The sensor noise is assumed to be additive and zero mean circularly symmetric complex Gaussian distributed, and independent of the source signals;

3) In order to avoid the phase ambiguity of $2\gamma_{xl}$ or $2\gamma_{yl}$ estimated later, the centro-symmetric cross array with element spacing $d \leq \lambda/4$ is required (see Paragraph 1 of Part B in Section 3, or see [26, 29] for details);

4) $2\gamma_{yp} - 2\gamma_{xp} \neq 2\gamma_{yq} - 2\gamma_{xq} + 2h\pi,\ h \in \{-1, 0, 1\},$ or $2\sqrt{2}d \sin\alpha_p \cos(\beta_p + \frac{\pi}{4}) \neq 2\sqrt{2}d \sin\alpha_q \cos(\beta_q + \frac{\pi}{4}) + h\lambda,\ p, q \in \{1, \ldots, L\}$ for $p \neq q$ is required to uniquely distinguish the introduced L phase angles (see the parts between (39) and (40), and between (46) and (47) in Section 3 for detailed analyses);

5) In this paper, the source number $L < 2N + 1$ is required, given a centro-symmetric two-dimensional cross-array[§] with $4N + 1$ sensors.

3. PROPOSED ALGORITHM

Note that the quadratic phase of near-field sources is a nonlinear function of (α_l, β_l, r_l), as shown in Eq. (16). An alternative indirect method for estimating (α_l, β_l, r_l) is to firstly obtain four matched intermediate parameters $(\gamma_{xl}, \phi_{xl}, \gamma_{yl}, \phi_{yl})$ and then solve Eqs. (5)–(8).

To obtain $(\gamma_{xl}, \phi_{xl}, \gamma_{yl}, \phi_{yl})$ by applying the conventional high-resolution search-free algorithm, it is necessary to transform the quadratic phase inherent in the near-field signal model into a linear phase. Note that the common characteristics of near-field and far-field sources consist in that $\gamma_{xl} \neq 0$ and $\gamma_{yl} \neq 0$, and their difference lies in that $(\phi_{xl} \neq 0, \phi_{yl} \neq 0)$ for near-field sources but $(\phi_{xl} = 0, \phi_{yl} = 0)$ for far-field sources. In addition, the above-mentioned transformation should retain the linear phase characteristic inherent for far-field sources so that both near-field and far-field sources share the same linear phase form to facilitate the solution and allow the same computations.

3.1. Constructing a Special Cumulant Matrix C

Cumulants can extend the array aperture and form virtual sensors using their available multiple degrees of freedom [40–44]. Motivated by this, the cumulant is chosen as the key technique for achieving the above transform, i.e., changing the quadratic phase inherent in the

[§] The propagation delay associated with the lth source between the $(0, 0)$th and (j, m)th sensor has the following complicated form: $\tau = j\gamma_{xl} + j^2\phi_{xl} + m\gamma_{yl} + m^2\phi_{yl} - jmd^2 \sin^2\alpha_l \sin^2\beta_l/(\lambda r_l)$. Therefore, the sensors on the x and y axes (i.e., $(j, 0)$ and $(0, m)$) are selected to construct a cross array rather than rectangular array, which is helpful to simplify the phase form of near-field sources and develop search-free estimation algorithms (see Eq. (5) of [25] and Eq. (4) of [29] for details).

near-field signal model into linear one, and keeping the linear phase of the far-field signal model.

Define the fourth-order cumulants from the outputs of the sensors in Fig. 1 as follows:

$$\begin{aligned}
&\operatorname{cum}\left\{x_{m,0}(k), x_{n,0}^*(k), x_{0,0}(k), x_{p,q}^*(k)\right\} \\
= &\operatorname{cum}\left\{\sum_{l=1}^{L} s_l(k) e^{i(m\gamma_{xl}+m^2\phi_{xl})}, \left(\sum_{l=1}^{L} s_l(k) e^{i(n\gamma_{xl}+n^2\phi_{xl})}\right)^*,\right. \\
&\left.\sum_{l=1}^{L} s_l(k), \left(\sum_{l=1}^{L} s_l(k) e^{i(p\gamma_{xl}+p^2\phi_{xl}+q\gamma_{yl}+q^2\phi_{yl})}\right)^*\right\} \\
= &\sum_{l=1}^{L} e^{i\left\{[(m-n)]\gamma_{xl}+[(m^2-n^2)]\phi_{xl}\right\}} \operatorname{cum}\left\{s_l(t), s_l^*(t), s_l(t), s_l^*(t)\right\} \\
&\times e^{-i(p\gamma_{xl}+p^2\phi_{xl}+q\gamma_{yl}+q^2\phi_{yl})} \\
= &\sum_{l=1}^{L} e^{i\left\{[(m-n)]\gamma_{xl}+[(m^2-n^2)]\phi_{xl}\right\}} c_{4,sl} e^{-i(p\gamma_{xl}+p^2\phi_{xl}+q\gamma_{yl}+q^2\phi_{yl})} \\
&m, n \in \{-N, -N+1, \ldots, -1, 1, 2, \ldots, N, 0\}, \\
&(p,q) \in \left\{\begin{array}{l}(-N,0), \ldots, (-1,0), (1,0), \ldots, (N,0), \\ (0,-N), \ldots, (0,-1), (0,1), \ldots, (0,N), (0,0)\end{array}\right\}, \qquad (18)
\end{aligned}$$

where $c_{4,sl} = \operatorname{cum}\{s_l(t), s_l^*(t), s_l(t), s_l^*(t)\}$ is the kurtosis of the lth signal, and the superscript $(\,)^*$ denotes the complex conjugate.

To retain the linear phase term (i.e., the common term γ_{xl} in both the near-field and far-field signal models) and to remove the quadratic phase term (i.e., the term ϕ_{xl} only in the near-field signal model) in $\exp\left\{i\left\{[(m-n)]\gamma_{xl}+[(m^2-n^2)]\phi_{xl}\right\}\right\}$, both $m-n \neq 0$ and $m^2-n^2=0$ are required. Let $n=-m$, and Eq. (18) becomes

$$\begin{aligned}
&\operatorname{cum}\{x_{m,0}(k), x_{-m,0}^*(k), x_{0,0}(k), x_{p,q}^*(k)\} \\
= &\sum_{l=1}^{L} e^{i\{2m\gamma_{xl}\}} c_{4,sl} e^{-i(p\gamma_{xl}+p^2\phi_{xl}+q\gamma_{yl}+q^2\phi_{yl})} \\
&m \in \{-N, -N+1, \ldots, -1, 1, 2, \ldots, N, 0\} \\
&(p,q) \in \left\{\begin{array}{l}(-N,0), \ldots, (-1,0), (1,0), \ldots, (N,0), \\ (0,-N), \ldots, (0,-1), (0,1), \ldots, (0,N), (0,0),\end{array}\right\}. \qquad (19)
\end{aligned}$$

Since there are $(2N+1)$ and $(4N+1)$ possible values for m and (p,q) respectively, we define two functions $h = g_1(m)$ and $j = g_2((p,q))$

to represent the following unique mappings:

$$\begin{cases} m = -N, -N+1, \ldots, -1 \Leftrightarrow h = g_1(m) = 1, 2, \ldots, N \\ m = 1, 2, \ldots, N \Leftrightarrow h = g_1(m) = N+1, N+2, \ldots, 2N \\ m = 0 \Leftrightarrow h = g_1(m) = 2N+1 \end{cases}, \quad (20)$$

and

$$\begin{cases} (p,q) = (-N,0), (-N+1,0), \ldots, (-1,0) \\ \qquad \Leftrightarrow j = g_2((p,q)) = 1, 2, \ldots, N \\ (p,q) = (1,0), (2,0), \ldots, (N,0) \\ \qquad \Leftrightarrow j = g_2((p,q)) = N+1, N+2, \ldots, 2N \\ (p,q) = (0,0) \Leftrightarrow j = g_2((p,q)) = 2N+1 \\ (p,q) = (0,-N), (0,-N+1), \ldots, (0,-1) \\ \qquad \Leftrightarrow j = g_2((p,q)) = 2N+2, 2N+3, \ldots, 3N+1 \\ (p,q) = (0,1), (0,2), \ldots, (0,N) \\ \qquad \Leftrightarrow j = g_2((p,q)) = 3N+2, 3N+3, \ldots, 4N+1 \end{cases}. \quad (21)$$

Based on Eqs. (19)–(21), we define a special cumulant matrix $\mathbf{C}_1$ (its rows and columns are indexed by h and j, respectively), whose (h,j)th element can be given by

$$\mathbf{C}_1(h,i) = \mathrm{cum}\left\{x_{g_1^{-1}(h),0}(k), x^*_{-g_1^{-1}(h),0}(k), x_{0,0}(k), x^*_{g_2^{-1}(j)}(k)\right\}$$
$$h \in \{1, 2, \ldots, 2N+1\}, \quad j \in \{1, 2, \ldots, 4N+1\}, \quad (22)$$

where $g_1^{-1}(h)$ and $g_2^{-1}(j)$ represent the inverse functions of $h = g_1(m)$ and $j = g_2((p,q))$, respectively.

Note that the $(2N+1) \times (4N+1)$-dimensional cumulant matrix $\mathbf{C}_1$ can be represented in a compact form as:

$$\mathbf{C}_1 = \mathbf{B}_1 \mathbf{C}_{4s} \mathbf{A}^H, \quad (23)$$

where the physical steering matrix $\mathbf{A}$ is defined in Eq. (15), $\mathbf{C}_{4s} = \mathrm{diag}[c_{4,s1}, c_{4,s2}, \ldots, c_{4,sL}]$, $\mathbf{B}_1 = [\mathbf{b}_1(\gamma_{x1})\ \mathbf{b}_1(\gamma_{x2}) \ldots \mathbf{b}_1(\gamma_{xL})]$, and $(2N+1) \times 1$-dimensional column vector

$$\mathbf{b}_1(\gamma_{xl}) = \left[e^{-i2N\gamma_{xl}}\ e^{-i2(N-1)\gamma_{xl}} \ldots e^{-i2\gamma_{xl}}\ e^{i2\gamma_{xl}} \ldots e^{i2(N-1)\gamma_{xl}}\ e^{i2N\gamma_{xl}}\ 1\right]^T,$$
$$l = 1, 2, \ldots, L. \quad (24)$$

Similar to Eq. (19), we define

$$\mathrm{cum}\left\{x_{0,m}(k), x^*_{0,-m}(k), x_{0,0}(k), x^*_{p,q}(k)\right\}$$
$$= \sum_{l=1}^{L} e^{i\left\{2m\gamma_{yl}\right\}} c_{4,sl} e^{-i(p\gamma_{xl} + p^2\phi_{xl} + q\gamma_{yl} + q^2\phi_{yl})}$$
$$m \in \{-N, -N+1, \ldots, -1, 1, 2, \ldots, N\},$$
$$(p,q) \in \left\{ \begin{array}{l} (-N,0), \ldots, (-1,0), (1,0), \ldots, (N,0), \\ (0,-N), \ldots, (0,-1), (0,1), \ldots, (0,N), (0,0), \end{array} \right\}, \quad (25)$$

where $m \neq 0$ is required to avoid the duplication of $m = 0$ in Eq. (19). Similar to Eq. (22), we define a special cumulant matrix $\mathbf{C}_2$, whose (h, j)th element can be given by

$$\mathbf{C}_2(h,j) = \mathrm{cum}\left\{x_{0,g_1^{-1}(h)}(k), x^*_{0,-g_1^{-1}(h)}(k), x_{0,0}(k), x^*_{g_2^{-1}(i)}(k)\right\} \quad h \in \{1,2,\ldots,2N\}, \quad j \in \{1,2,\ldots,4N+1\}, \quad (26)$$

where $h \neq 2N+1$ is required to avoid the duplication of $m = 0$ in Eq. (19). Note that the $(2N) \times (4N+1)$-dimensional cumulant matrix $\mathbf{C}_2$ can be represented in a compact form as:

$$\mathbf{C}_2 = \mathbf{B}_2 \mathbf{C}_{4s} \mathbf{A}^H, \quad (27)$$

where $\mathbf{B}_2 = [\mathbf{b}_2(\gamma_{y1})\ \mathbf{b}_2(\gamma_{y2}) \ldots \mathbf{b}_2(\gamma_{yL})]$, and $(2N) \times 1$-dimensional column vector

$$\mathbf{b}_2(\gamma_{yl}) = [e^{-i2N\gamma_{yl}}\ e^{-i2(N-1)\gamma_{yl}} \ldots e^{-i2\gamma_{yl}}\ e^{i2\gamma_{yl}} \ldots e^{i2(N-1)\gamma_{yl}}\ e^{i2N\gamma_{yl}}]^T, \quad l = 1,2,\ldots,L. \quad (28)$$

Combining $\mathbf{C}_1$ and $\mathbf{C}_2$, we construct a $(4N+1) \times (4N+1)$-dimensional cumulant matrix $\mathbf{C}$:

$$\mathbf{C} = \begin{bmatrix} \mathbf{C}_1 \\ \mathbf{C}_2 \end{bmatrix} = \mathbf{B}\mathbf{C}_{4s}\mathbf{A}^H, \quad (29)$$

where the virtual steering matrix

$$\mathbf{B} = \begin{bmatrix} \mathbf{B}_1 \\ \mathbf{B}_2 \end{bmatrix} = [\mathbf{b}(\gamma_{x1},\gamma_{y1})\ \mathbf{b}(\gamma_{x2},\gamma_{y2}) \ldots \mathbf{b}(\gamma_{xL},\gamma_{yL})], \quad (30)$$

and the virtual steering vector

$$\mathbf{b}(\gamma_{xl},\gamma_{yl}) = \left[\mathbf{b}_1^T(\gamma_{xl})\ \mathbf{b}_2^T(\gamma_{yl})\right]^T, \quad l = 1,2,\ldots,L. \quad (31)$$

Note that the cumulant matrix $\mathbf{C}$ has the following characteristics:

1) The cumulant matrix $\mathbf{C}$ is the product of three components, i.e., the virtual steering matrix $\mathbf{B}$, the diagonal matrix $\mathbf{C}_{4s}$, and the conjugate transpose of the physical steering matrix $\mathbf{A}$;
2) On the virtual steering matrix $\mathbf{B}$: The virtual steering matrix $\mathbf{B}$ contains linear phase terms rather than the quadratic phase terms of the physical steering matrix. In addition, $\mathbf{B}$ has full column rank for "arbitrary"-field sources. Furthermore, no matter whether the lth source be in the far-field or in the near-field, the virtual steering vector $\mathbf{b}(\gamma_{xl},\gamma_{yl})$ has the same form, i.e., the linear phase term is a function of the two common intermediate parameters (γ_x,γ_y) in both near-field and far-field signal models. The first intuition is to obtain $(\gamma_{xl},\gamma_{yl})$ from the restored virtual steering vector $\mathbf{b}(\gamma_{xl},\gamma_{yl})$ and then solve the azimuth-elevation

arrival-angles (α_l, β_l) of the lth (near-field or far-field) source independent of r_l using $(\gamma_{xl}, \gamma_{yl})$. The remaining problem is how to restore the virtual steering vector $\mathbf{b}(\gamma_{xl}, \gamma_{yl})$.

3) On the physical steering matrix $\mathbf{A}$: Note that $\mathbf{A}$ contains the range information (or two intermediate parameters (ϕ_x, ϕ_y)) of near-field sources. Therefore, the ranges of near-field sources can be obtained from $\mathbf{A}$. Another intuition is to obtain (ϕ_{xl}, ϕ_{yl}) from the restored physical steering vector $\mathbf{a}(\gamma_{xl}, \phi_{xl}, \gamma_{yl}, \phi_{yl})$ and then estimate the range of the lth near-field source from (ϕ_{xl}, ϕ_{yl}). The remaining problem is how to restore the physical steering vector $\mathbf{a}(\gamma_{xl}, \phi_{xl}, \gamma_{yl}, \phi_{yl})$.

To facilitate the derivation of the two-stage separated steering vector-based algorithm, we implement the singular value decomposition (SVD) of $(4N+1) \times (4N+1)$-dimensional cumulant matrix $\mathbf{C}$ as follows:

$$\begin{aligned}\mathbf{C} &= \mathbf{B}\mathbf{C}_{4s}\mathbf{A}^H = \mathbf{U}\mathbf{\Sigma}\mathbf{V}^H = \mathbf{U}_s\mathbf{\Sigma}_s\mathbf{V}_s^H + \mathbf{U}_n\mathbf{\Sigma}_n\mathbf{V}_n^H \\ &= [\mathbf{u}_1, \ldots, \mathbf{u}_{4N+1}]\mathrm{diag}[\sigma_1, \ldots, \sigma_{4N+1}][\mathbf{v}_1, \ldots, \mathbf{v}_{4N+1}]^H, \quad (32)\end{aligned}$$

where $\mathbf{\Sigma}$ is the diagonal matrix with the singular values arranged as $|\sigma_1| \geq \ldots \geq |\sigma_L| > |\sigma_{L+1}| \geq \ldots \geq |\sigma_{4N+1}|$, the diagonal matrix $\mathbf{\Sigma}_s \in R^{L\times L}$ is composed of singular values $\sigma_1, \sigma_2, \ldots, \sigma_L$, and $\mathbf{U}_s \in C^{(4N+1)\times L}$ consists of the left singular vectors $\mathbf{u}_1, \mathbf{u}_2, \ldots, \mathbf{u}_L$ related to $\sigma_1, \sigma_2, \ldots, \sigma_L$ In addition, $\mathbf{V}_s \in C^{(4N+1)\times L}$, which spans the same range as that of the physical steering matrix $\mathbf{A}$, consists of the right singular vectors $\mathbf{v}_1, \mathbf{v}_2, \ldots, \mathbf{v}_L$ related to $\sigma_1, \sigma_2, \ldots, \sigma_L$. Similarly, the diagonal matrix $\mathbf{\Sigma}_n \in R^{(4N+1-L)\times(4N+1-L)}$ is composed of singular values $\sigma_{L+1}, \sigma_{L+2}, \ldots, \sigma_{4N+1}$; $\mathbf{U}_n \in C^{(4N+1)\times(4N+1-L)}$ consists of the left singular vectors $\mathbf{u}_{L+1}, \mathbf{u}_{L+2}, \ldots, \mathbf{u}_{4N+1}$ related to $\sigma_{L+1}, \sigma_{L+2}, \ldots, \sigma_{4N+1}$, orthogonal to the range space of $\mathbf{B}$. $\mathbf{V}_n \in C^{(4N+1)\times(4N+1-L)}$, consists of the right singular vectors $\mathbf{v}_{L+1}, \mathbf{v}_{L+2}, \ldots, \mathbf{v}_{4N+1}$ related to $\sigma_{L+1}, \sigma_{L+2}, \ldots, \sigma_{4N+1}$, orthogonal to the range space of $\mathbf{A}$.

3.2. Estimating (α_l, β_l) by Introducing θ_l, Separating the Virtual Steering Vector $\mathbf{b}(\gamma_{xl}, \gamma_{yl})$ into Two Parts, and Restoring $\mathbf{b}(\gamma_{xl}, \gamma_{yl})$

$\mathbf{b}(\gamma_{xl}, \gamma_{yl}) = \left[\mathbf{b}_1^T(\gamma_{xl})\ \mathbf{b}_2^T(\gamma_{yl})\right]^T$ can be considered as the steering vector of the lth virtual far-field source observed by a cross array with uniform element spacing $2d$, resulting in bigger element spacing in cumulant domain than that of the physical array (d). Therefore,

Assumption 3 in Part II is required to avoid the phase ambiguity for $2\gamma_{xl}$ and $2\gamma_{yl}$.

Although many high-resolution methods can be utilized to estimate phase vectors $\{\gamma_{x1}, \gamma_{x2}, \ldots, \gamma_{xL}\}$ and $\{\gamma_{y1}, \gamma_{y2}, \ldots, \gamma_{yL}\}$ separately [5–10], Eqs. (5) and (7) cannot be solved for azimuth-elevation arrival-angles without the knowledge of the relative orders of the vector elements. Consequently, any method for estimating multi-dimensional source parameters should address the pairing problem since the failure in pairing will cause severe performance degradation [6–10]. For example, if the parameter (γ_{xp}) of the pth source and the parameter (γ_{yq}) of the qth source are falsely associated, $(\gamma_{xp}, \gamma_{yq})$ will result in wrong estimation and severe performance degradation for azimuth-elevation arrival-angles. Since the cross array consists of two orthogonal subarrays which results in no direct association between $\{\gamma_{x1}, \gamma_{x2}, \ldots, \gamma_{xL}\}$ and $\{\gamma_{y1}, \gamma_{y2}, \ldots, \gamma_{yL}\}$, pairing them is a key problem in the proposed algorithm. To avoid any matching operation, we consider estimating γ_{xl} and γ_{yl} from the restored virtual steering vector $\mathbf{b}(\gamma_{xl}, \gamma_{yl})$.

Define

$$z_l = e^{i2\gamma_{yl}} / e^{i2\gamma_{xl}} = e^{i2(\gamma_{yl} - \gamma_{xl})}, \quad l = 1, \ldots, L. \tag{33}$$

Since $|z_l| = 1$, z_l can be represented in another form as:

$$z_l = e^{i\theta_l}, \quad \theta_l \in [-\pi, \pi], \quad l = 1, \ldots, L. \tag{34}$$

Although $e^{i\theta_l} = e^{i2(\gamma_{yl} - \gamma_{xl})}$, θ_l may not equal $2(\gamma_{yl} - \gamma_{xl})$ due to $2\gamma_{yl}$, $2\gamma_{xl} \in [-\pi, \pi]$ (see Eqs. (5)–(7) and Assumption 3 in Section 2) and thus $2(\gamma_{yl} - \gamma_{xl})$ may exceed $[-\pi, \pi]$, i.e., $2(\gamma_{yl} - \gamma_{xl})$ cannot be estimated from θ_l directly, but $e^{i2(\gamma_{yl} - \gamma_{xl})}$ can be estimated from $e^{i\theta_l}$ uniquely (see Assumption 4 in Section 2).

Based on Eqs. (33) and (34), $e^{i2\gamma_{yl}}$ can be represented as $e^{i2\gamma_{yl}} = e^{i\theta_l} e^{i2\gamma_{xl}}$. Therefore, the virtual steering vector $\mathbf{b}(\gamma_{xl}, \gamma_{yl})$ in Eq. (31) can be written in another form as:

$$\begin{aligned}
&\mathbf{b}(\gamma_{xl}, \gamma_{yl}) \\
&= \Big[e^{-i2N\gamma_{xl}} \; e^{-i2(N-1)\gamma_{xl}} \; \ldots \; e^{-i2\gamma_{xl}} \; e^{i2\gamma_{xl}} \; \ldots \; e^{i2(N-1)\gamma_{xl}} \; e^{i2N\gamma_{xl}} \; 1 \\
&\quad e^{-i2N\gamma_{xl}} \times e^{-iN\theta_l} \; e^{-i2(N-1)\gamma_{xl}} \times e^{-i(N-1)\theta_l} \ldots e^{-i2\gamma_{xl}} \times e^{-i\theta_l} \; e^{i2\gamma_{xl}} \\
&\quad \times e^{i\theta_l} \ldots \; e^{i2(N-1)\gamma_{xl}} \times e^{i(N-1)\theta_l} \; e^{i2N\gamma_{xl}} \times e^{iN\theta_l} \Big]^T .
\end{aligned} \tag{35}$$

It is noted that no related factor exists between the first $2N$ elements and the last $2N$ elements in Eq. (31) (Or see Eqs. (24) and (28) for details). However, there is a related factor $e^{j\theta_l}$ between the first $2N$ elements and the last $2N$ elements in Eq. (35). In such case,

an alternative method for estimating $(\gamma_{xl}, \gamma_{yl})$ is to firstly estimate (θ_l, γ_{xl}) from Eq. (35) and then combine θ_l and γ_{xl}, yielding γ_{yl}.

Since $\mathbf{U_s}$ spans the same range as that of the virtual steering matrix $\mathbf{B}$, there must exist a unique invertible matrix $\mathbf{T}$, such that $\mathbf{U_s} = \mathbf{BT}$ [5]. To estimate θ_l, we implement the following divisions:

$$\begin{aligned}\mathbf{U_s} &= \begin{bmatrix} \mathbf{U}_1 \\ Last\ (2N+1)\ rows\ of\ \mathbf{U_s} \end{bmatrix} = \begin{bmatrix} First\ (2N+1)\ rows\ of\ \mathbf{U_s} \\ \mathbf{U}_2 \end{bmatrix} \\ &= \mathbf{BT} = \begin{bmatrix} \bar{\mathbf{B}}_1 \\ Last\ (2N+1)\ rows\ of\ \mathbf{B} \end{bmatrix} \mathbf{T} \\ &= \begin{bmatrix} First\ (2N+1)\ rows\ of\ \mathbf{B} \\ \mathbf{B}_2 \end{bmatrix} \mathbf{T}, \end{aligned} \tag{36}$$

where $\mathbf{U}_1$ and $\bar{\mathbf{B}}_1$ (i.e., the first $2N$ rows of $\mathbf{B}_1$) are the first $2N$ rows of $\mathbf{U_s}$ and $\mathbf{B}$, respectively. $\mathbf{U}_2$ and $\mathbf{B}_2$ are the last $2N$ rows of $\mathbf{U_s}$ and $\mathbf{B}$, respectively.

Similar to the generalized ESPRIT algorithm for one-dimensional arrival-angle estimation [45], we define a matrix

$$\mathbf{\Psi}(e^{i\theta})\mathbf{U}_1 - \mathbf{U}_2 = \left(\mathbf{\Psi}(e^{i\theta})\bar{\mathbf{B}}_1 - \mathbf{B}_2\right)\mathbf{T}, \tag{37}$$

where

$$\begin{aligned}\mathbf{\Psi}(e^{i\theta}) \;=\; \mathrm{diag}\Big\{ & e^{-iN\theta}, e^{-i(N-1)\theta}, \ldots, e^{-i\theta}, \\ & e^{i\theta}, \ldots, e^{i(N-1)\theta}, e^{iN\theta} \Big\}. \end{aligned} \tag{38}$$

From Eqs. (37) and (38), we can see that when $e^{i\theta} = e^{i2(\gamma_{yl}-\gamma_{xl})}$, the lth column of the matrix $\mathbf{\Psi}(e^{i\theta})\bar{\mathbf{B}}_1 - \mathbf{B}_2$ changes to zero. In such case, $\mathbf{\Psi}(e^{i\theta})\bar{\mathbf{B}}_1 - \mathbf{B}_2$ will drop rank. As $\bar{\mathbf{B}}_1$ and $\mathbf{B}_2$ are tall matrices, we can obtain the estimate of $e^{i2(\gamma_{yl}-\gamma_{xl})}$ for which $L \times L$-dimensional matrix $\left(\mathbf{\Psi}(e^{i\theta})\mathbf{U}_1 - \mathbf{U}_2\right)^H \left(\mathbf{\Psi}(e^{i\theta})\mathbf{U}_1 - \mathbf{U}_2\right)$ drops rank, i.e., rank $\left((\mathbf{\Psi}(e^{i\theta})\mathbf{U}_1 - \mathbf{U}_2)^H(\mathbf{\Psi}(e^{i\theta})\mathbf{U}_1 - \mathbf{U}_2)\right) < L$. Or equivalently the polynomial of $e^{i\theta}$ equals zero, as shown in the following equation:

$$P\left(e^{i\theta}\right) = \det\left\{\left(\mathbf{\Psi}\left(e^{i\theta}\right)\mathbf{U}_1 - \mathbf{U}_2\right)^H \left(\mathbf{\Psi}\left(e^{i\theta}\right)\mathbf{U}_1 - \mathbf{U}_2\right)\right\} = 0. \tag{39}$$

Therefore, $e^{i\hat{\theta}_l}$ can be found from the L roots of $P(e^{i\theta})$, which are located closest to the unit circle [45, 46].

When $2\gamma_{yp} - 2\gamma_{xp} = 2\gamma_{yq} - 2\gamma_{xq} + 2h\pi$, $h \in \{-1, 0, 1\}$, $p, q \in \{1, \ldots, L\}$ or $2\sqrt{2}d\sin\alpha_p\cos(\beta_p + \frac{\pi}{4}) = 2\sqrt{2}d\sin\alpha_q\cos(\beta_q + \frac{\pi}{4}) + h\lambda$ holds for the pth and qth sources, $e^{i2(\gamma_{yp}-\gamma_{xp})} = e^{i2(\gamma_{yq}-\gamma_{xq})}$ and $\theta_p = \theta_q$.

Therefore, it is difficult to distinguish the introduced L phase angles $\{\theta_1, \theta_2, \ldots, \theta_L\}$ uniquely using the objective function in Eq. (39) when $2\gamma_{yp} - 2\gamma_{xp} = 2\gamma_{yq} - 2\gamma_{xq} + 2h\pi$. It is clear that Assumption 4 in Section 2 is required to ensure that the objective function in Eq. (39) can distinguish the introduced L phase angles $\{\theta_1, \theta_2, \ldots, \theta_L\}$ as well as the L sources uniquely.

Let us consider the conventional spectral MUSIC algorithm [4] that estimates the parameters $\{\gamma_{xl}, \gamma_{yl}\}$, $l = 1, \ldots, L$ from the L deepest minima of the following function

$$f_2(\gamma_x, \gamma_y) = \mathbf{b}^H(\gamma_x, \gamma_y)\mathbf{U}_n\mathbf{U}_n^H\mathbf{b}(\gamma_x, \gamma_y). \tag{40}$$

Note that the virtual steering vector $\mathbf{b}(\gamma_x, \gamma_y)$ can be represented in a separate form as:

$$\mathbf{b}(\gamma_x, \gamma_y) = \mathbf{B}_3\left(e^{j\theta}\right)\mathbf{b}_4(\gamma_x), \tag{41}$$

where

$$\begin{aligned}\mathbf{b}_4(\gamma_x) = \Big[&\left(e^{i2\gamma_x}\right)^{-N} \quad \left(e^{i2\gamma_x}\right)^{-(N-1)} \quad \ldots \quad \left(e^{i2\gamma_x}\right)^{-1} \\ &\left(e^{i2\gamma_x}\right) \quad \ldots \quad \left(e^{i2\gamma_x}\right)^{(N-1)} \quad \left(e^{i2\gamma_x}\right)^{N} \quad 1\Big]^T,\end{aligned} \tag{42}$$

and

$$\mathbf{B}_3(e^{i\theta}) = \begin{bmatrix} \mathbf{I}_{2N+1} \\ \mathbf{\Psi}(e^{i\theta})\ \mathbf{0}_{2N\times 1} \end{bmatrix}. \tag{43}$$

Inserting (41) into (40), we have

$$\begin{aligned} & f_2(\gamma_x, \gamma_y) \\ = \ & \mathbf{b}_4^H(\gamma_x)\mathbf{B}_3^H\left(e^{i\theta}\right)\mathbf{U}_n\mathbf{U}_n^H\mathbf{B}_3\left(e^{i\theta}\right)\mathbf{b}_4(\gamma_x) \\ = \ & \mathbf{b}_4^H(\gamma_x)\mathbf{D}_1(e^{i\theta})\mathbf{b}_4(\gamma_x), \end{aligned} \tag{44}$$

where

$$\mathbf{D}_1\left(e^{i\theta}\right) = \mathbf{B}_3^H\left(e^{i\theta}\right)\mathbf{U}_n\mathbf{U}_n^H\mathbf{B}_3\left(e^{i\theta}\right) \tag{45}$$

is a $(2N+1)\times(2N+1)$-dimensional Hermitian matrix.

Equations (40) and (44) imply that: substituting the estimate $e^{i\hat{\theta}_l}$ into $\mathbf{B}_3(e^{i\theta})$ in (40), then finding the minima of the following objective function:

$$\hat{\gamma}_{xl} = \min_{\gamma_x}\ \mathbf{b}_4^H(\gamma_x)\mathbf{D}_1\left(e^{i\hat{\theta}_l}\right)\mathbf{b}_4(\gamma_x), \tag{46}$$

the minima of which indicates the estimate $\hat{\gamma}_{xl}$.

When $2\gamma_{yp} - 2\gamma_{xp} = 2\gamma_{yq} - 2\gamma_{xq} + 2h\pi$, $h \in \{-1, 0, 1\}$, $p, q \in \{1, \ldots, L\}$, i.e., $e^{i2(\gamma_{yp}-\gamma_{xp})} = e^{i2(\gamma_{yq}-\gamma_{xq})}$ and $\theta_p = \theta_q$, we have

$\mathbf{b}_4^H(\gamma_{xq})\,\mathbf{D}_1(e^{i\theta_q})\mathbf{b}_4(\gamma_{xq}) = \mathbf{b}_4^H(\gamma_{xp})\,\mathbf{D}_1(e^{i\theta_q})\mathbf{b}_4(\gamma_{xp})$ which implies that $\mathbf{b}_4^H(\gamma_x)\,\mathbf{D}_1(e^{i\theta_q})\mathbf{b}_4(\gamma_x)$ has not unique but two minimal values at $\gamma_x = \gamma_{xp}$ and $\gamma_x = \gamma_{xq}$. Therefore, Assumption 4 in Section 2 is required to ensure that $\mathbf{b}_4^H(\gamma_x)\,\mathbf{D}_1(e^{i\theta_q})\mathbf{b}_4(\gamma_x)$ in Eq. (46) has unique minimal value.

Additionally, Eq. (46) implies that $\mathbf{b}_4(\hat{\gamma}_{x_l})$ is just the eigenvector corresponding to the smallest eigenvalue of $\mathbf{D}_1(e^{i\hat{\theta}_l})$.

Once $\mathbf{b}_4(\hat{\gamma}_{x_l})$ is obtained from the EVD of $\mathbf{D}_1(e^{i\hat{\theta}_l})$, $\mathbf{b}(\hat{\gamma}_{xl},\hat{\gamma}_{yl})$ is easily restored from the following equation:

$$\mathbf{b}(\hat{\gamma}_{xl},\hat{\gamma}_{yl}) = \mathbf{B}_3\left(e^{i\hat{\theta}_l}\right)\mathbf{b}_4(\hat{\gamma}_{xl})\,. \tag{47}$$

Based on $\mathbf{b}(\hat{\gamma}_{xl},\hat{\gamma}_{yl})$ and its linear phase characteristic, the estimates $(\hat{\gamma}_{xl},\hat{\gamma}_{yl})$ can be given as follows:

$$\begin{aligned}\hat{\gamma}_{xl} &= \frac{1}{4N}\left\{\sum_{j=1}^{N-1}\angle\left(\frac{\mathbf{b}(\hat{\gamma}_{xl},\hat{\gamma}_{yl})[j+1]}{\mathbf{b}(\hat{\gamma}_{xl},\hat{\gamma}_{yl})[j]}\right)+\angle\left(\frac{\mathbf{b}(\hat{\gamma}_{xl},\hat{\gamma}_{yl})[2N+1]}{\mathbf{b}(\hat{\gamma}_{xl},\hat{\gamma}_{yl})[N]}\right)\right.\\ &\left.+\sum_{j=N+1}^{2N-1}\angle\left(\frac{\mathbf{b}(\hat{\gamma}_{xl},\hat{\gamma}_{yl})[j+1]}{\mathbf{b}(\hat{\gamma}_{xl},\hat{\gamma}_{yl})[j]}\right)+\angle\left(\frac{\mathbf{b}(\hat{\gamma}_{xl},\hat{\gamma}_{yl})[N+1]}{\mathbf{b}(\hat{\gamma}_{xl},\hat{\gamma}_{yl})[2N+1]}\right)\right\},\end{aligned} \tag{48}$$

$$\begin{aligned}\hat{\gamma}_{yl} &= \frac{1}{4N}\left\{\sum_{j=2N+2}^{3N}\angle\left(\frac{\mathbf{b}(\hat{\gamma}_{xl},\hat{\gamma}_{yl})[j+1]}{\mathbf{b}(\hat{\gamma}_{xl},\hat{\gamma}_{yl})[j]}\right)+\angle\left(\frac{\mathbf{b}(\hat{\gamma}_{xl},\hat{\gamma}_{yl})[2N+1]}{\mathbf{b}(\hat{\gamma}_{xl},\hat{\gamma}_{yl})[3N+1]}\right)\right.\\ &\left.+\sum_{j=3N+2}^{4N}\angle\left(\frac{\mathbf{b}(\hat{\gamma}_{xl},\hat{\gamma}_{yl})[j+1]}{\mathbf{b}(\hat{\gamma}_{xl},\hat{\gamma}_{yl})[j]}\right)+\angle\left(\frac{\mathbf{b}(\hat{\gamma}_{xl},\hat{\gamma}_{yl})[3N+2]}{\mathbf{b}(\hat{\gamma}_{xl},\hat{\gamma}_{yl})[2N+1]}\right)\right\},\end{aligned} \tag{49}$$

where $\mathbf{b}(\hat{\gamma}_{xl},\hat{\gamma}_{yl})[j]$ denotes the jth element of the vector $\mathbf{b}(\hat{\gamma}_{xl},\hat{\gamma}_{yl})$.

Based on $(\hat{\gamma}_{xl},\hat{\gamma}_{yl})$, α_l and β_l can be solved from Eqs. (5) and (7) as follows:

$$\hat{\alpha}_l = \arcsin\left(\frac{\lambda}{2\pi d}\sqrt{\hat{\gamma}_{xl}^2+\hat{\gamma}_{yl}^2}\right), \tag{50}$$

$$\hat{\beta}_l = \arctan\left(\frac{\hat{\gamma}_{yl}}{\hat{\gamma}_{xl}}\right). \tag{51}$$

3.3. Estimating r_l by Separating the Physical Steering Vector $\mathbf{a}(\gamma_x,\phi_x,\gamma_y,\phi_y)$ into Two Parts, and Restoring $\mathbf{a}_2(\phi_{xl},\phi_{yl})$

Let us consider the conventional spectral MUSIC algorithm [4] that estimates the four-dimensional parameters $(\gamma_{xl},\phi_{xl},\gamma_{yl},\phi_{yl})$ from the

L deepest minima of the following objective function:

$$f_3(\gamma_x, \phi_x, \gamma_y, \phi_y) = \mathbf{a}^H(\gamma_x, \phi_x, \gamma_y, \phi_y)\mathbf{V}_n\mathbf{V}_n^H\mathbf{a}(\gamma_x, \phi_x, \gamma_y, \phi_y), \quad (52)$$

Note that the physical steering vector $\mathbf{a}(\gamma_x, \phi_x, \gamma_y, \phi_y)$ can be represented in a separate form as:

$$\mathbf{a}(\gamma_x, \phi_x, \gamma_y, \phi_y) = \mathbf{A}_1(\gamma_x, \gamma_y)\mathbf{a}_2(\phi_x, \phi_y), \quad (53)$$

where the second part

$$\mathbf{a}_2(\phi_x, \phi_y) = \left[e^{iN^2\phi_x}\ e^{i(N-1)^2\phi_x}\ \ldots\ e^{i\phi_x}\ 1\ \ e^{iN^2\phi_y}\ e^{i(N-1)^2\phi_y}\ \ldots\ e^{i\phi_y}\right]^T \quad (54)$$

and the first part

$$\mathbf{A}_1(\gamma_x, \gamma_y) = \begin{bmatrix} \mathbf{\Delta}_1 & \mathbf{0} & \mathbf{0} \\ \mathbf{\Delta}_2 & \mathbf{0} & \mathbf{0} \\ \mathbf{0} & 1 & \mathbf{0} \\ \mathbf{0} & \mathbf{0} & \mathbf{\Delta}_3 \\ \mathbf{0} & \mathbf{0} & \mathbf{\Delta}_4 \end{bmatrix}. \quad (55)$$

In Eq. (55),

$$\mathbf{\Delta}_1 = \mathrm{diag}\left\{\left(e^{i\gamma_x}\right)^{-N}, \left(e^{i\gamma_x}\right)^{-N+1}, \ldots, \left(e^{i\gamma_x}\right)^{-1}\right\}, \quad (56)$$

$$\mathbf{\Delta}_2 = \mathrm{adiag}\left\{\left(e^{i\gamma_x}\right)^{N}, \left(e^{i\gamma_x}\right)^{N-1}, \ldots, e^{i\gamma_x}\right\}, \quad (57)$$

$$\mathbf{\Delta}_3 = \mathrm{diag}\left\{\left(e^{i\gamma_y}\right)^{-N}, \left(e^{i\gamma_y}\right)^{-N+1}, \ldots, \left(e^{i\gamma_y}\right)^{-1}\right\}, \quad (58)$$

and

$$\mathbf{\Delta}_4 = \mathrm{adiag}\left\{\left(e^{i\gamma_y}\right)^{N}, \left(e^{i\gamma_y}\right)^{N-1}, \ldots, e^{i\gamma_y}\right\}. \quad (59)$$

Inserting (53) into (52), we have

$$\begin{aligned} & f_3(\gamma_x, \phi_x, \gamma_y, \phi_y) = \mathbf{a}^H(\gamma_x, \phi_x, \gamma_y, \phi_y)\mathbf{V}_n\mathbf{V}_n^H\mathbf{a}(\gamma_x, \phi_x, \gamma_y, \phi_y) \\ = & \ \mathbf{a}_2^H(\phi_x, \phi_y)\mathbf{A}_1^H(\gamma_x, \gamma_y)\mathbf{V}_n\mathbf{V}_n^H\mathbf{A}_1(\gamma_x, \gamma_y)\mathbf{a}_2(\phi_x, \phi_y) \\ = & \ \mathbf{a}_2^H(\phi_x, \phi_y)\mathbf{D}_2(\gamma_x, \gamma_y)\mathbf{a}_2(\phi_x, \phi_y), \end{aligned} \quad (60)$$

where

$$\mathbf{D}_2(\gamma_x, \gamma_y) = \mathbf{A}_1^H(\gamma_x, \gamma_y)\mathbf{V}_n\mathbf{V}_n^H\mathbf{A}_1(\gamma_x, \gamma_y) \quad (61)$$

is a $(2N+1) \times (2N+1)$-dimensional Hermitian matrix.

Equations (52) and (60) imply that: substituting estimates $(\hat{\gamma}_{xl}, \hat{\gamma}_{yl})$ into $\mathbf{A}_1(\gamma_x, \gamma_y)$ in (53), then finding the minima of the following objective function:

$$(\hat{\phi}_{xl}, \hat{\phi}_{yl}) = \min_{\phi_x, \phi_y} \mathbf{a}_2^H(\phi_x, \phi_y)\mathbf{D}_2(\hat{\gamma}_{xl}, \hat{\gamma}_{yl})\mathbf{a}_2(\phi_x, \phi_y), \quad (62)$$

the minima of which indicates the estimates $(\hat{\phi}_{xl}, \hat{\phi}_{yl})$.

Additionally, Eq. (62) implies that $\mathbf{a}_2(\hat{\phi}_{xl}, \hat{\phi}_{yl})$ is just the eigenvector corresponding to the smallest eigenvalue of $\mathbf{D}_2(\hat{\gamma}_{xl}, \hat{\gamma}_{yl})$. Therefore, $\mathbf{a}_2(\hat{\phi}_{xl}, \hat{\phi}_{yl})$ can be recovered from the EVD of $\mathbf{D}_2(\hat{\gamma}_{xl}, \hat{\gamma}_{yl})$.

Note that the phases in $\mathbf{a}_2(\hat{\phi}_{xl}, \hat{\phi}_{yl})$ are the quadratic functions of the sensor indexes i and m (See Eq. (54) for details). To transform the quadratic phases into linear ones and obtain $(\hat{\phi}_{xl}, \hat{\phi}_{yl})$ without spectral search, we form two column vectors from $\mathbf{a}_2(\hat{\phi}_{xl}, \hat{\phi}_{yl})$ as follows:

$$\begin{aligned}
\mathbf{e}_l &= \begin{bmatrix}
\hat{\mathbf{a}}_2(\hat{\phi}_{xl}, \hat{\phi}_{yl})[N]\hat{\mathbf{a}}_2^*(\hat{\phi}_{xl}, \hat{\phi}_{yl})[N+1]\hat{\mathbf{a}}_2^*(\hat{\phi}_{xl}, \hat{\phi}_{yl})[N]\hat{\mathbf{a}}_2(\hat{\phi}_{xl}, \hat{\phi}_{yl})[N+1] \\
\hat{\mathbf{a}}_2(\hat{\phi}_{xl}, \hat{\phi}_{yl})[N-1]\hat{\mathbf{a}}_2^*(\hat{\phi}_{xl}, \hat{\phi}_{yl})[N]\hat{\mathbf{a}}_2^*(\hat{\phi}_{xl}, \hat{\phi}_{yl})[N]\hat{\mathbf{a}}_2(\hat{\phi}_{xl}, \hat{\phi}_{yl})[N+1] \\
\hat{\mathbf{a}}_2(\hat{\phi}_{xl}, \hat{\phi}_{yl})[N-2]\hat{\mathbf{a}}_2^*(\hat{\phi}_{xl}, \hat{\phi}_{yl})[N-1]\hat{\mathbf{a}}_2^*(\hat{\phi}_{xl}, \hat{\phi}_{yl})[N]\hat{\mathbf{a}}_2(\hat{\phi}_{xl}, \hat{\phi}_{yl})[N+1] \\
\vdots \\
\hat{\mathbf{a}}_2(\hat{\phi}_{xl}, \hat{\phi}_{yl})[1]\hat{\mathbf{a}}_2^*(\hat{\phi}_{xl}, \hat{\phi}_{yl})[2]\hat{\mathbf{a}}_2^*(\hat{\phi}_{xl}, \hat{\phi}_{yl})[N]\hat{\mathbf{a}}_2(\hat{\phi}_{xl}, \hat{\phi}_{yl})[N+1]
\end{bmatrix} \\
&= \begin{bmatrix} 1 \\ e^{i2\hat{\phi}_{xl}} \\ e^{i4\hat{\phi}_{xl}} \\ \vdots \\ e^{i2(N-1)\hat{\phi}_{xl}} \end{bmatrix}, \qquad (63)
\end{aligned}$$

$$\begin{aligned}
\mathbf{f}_l &= \begin{bmatrix}
\hat{\mathbf{a}}_2(\hat{\phi}_{xl}, \hat{\phi}_{yl})[2N+1]\hat{\mathbf{a}}_2^*(\hat{\phi}_{xl}, \hat{\phi}_{yl})[N+1]\hat{\mathbf{a}}_2^*(\hat{\phi}_{xl}, \hat{\phi}_{yl})[2N+1]\hat{\mathbf{a}}_2(\hat{\phi}_{xl}, \hat{\phi}_{yl})[N+1] \\
\hat{\mathbf{a}}_2(\hat{\phi}_{xl}, \hat{\phi}_{yl})[2N]\hat{\mathbf{a}}_2^*(\hat{\phi}_{xl}, \hat{\phi}_{yl})[2N+1]\hat{\mathbf{a}}_2^*(\hat{\phi}_{xl}, \hat{\phi}_{yl})[2N+1]\hat{\mathbf{a}}_2(\hat{\phi}_{xl}, \hat{\phi}_{yl})[N+1] \\
\hat{\mathbf{a}}_2(\hat{\phi}_{xl}, \hat{\phi}_{yl})[2N-1]\hat{\mathbf{a}}_2^*(\hat{\phi}_{xl}, \hat{\phi}_{yl})[2N]\hat{\mathbf{a}}_2^*(\hat{\phi}_{xl}, \hat{\phi}_{yl})[2N+1]\hat{\mathbf{a}}_2(\hat{\phi}_{xl}, \hat{\phi}_{yl})[N+1] \\
\vdots \\
\hat{\mathbf{a}}_2(\hat{\phi}_{xl}, \hat{\phi}_{yl})[N+2]\hat{\mathbf{a}}_2^*(\hat{\phi}_{xl}, \hat{\phi}_{yl})[N+3]\hat{\mathbf{a}}_2^*(\hat{\phi}_{xl}, \hat{\phi}_{yl})[2N+1]\hat{\mathbf{a}}_2(\hat{\phi}_{xl}, \hat{\phi}_{yl})[N+1]
\end{bmatrix} \\
&= \begin{bmatrix} 1 \\ e^{i2\hat{\phi}_{yl}} \\ e^{i4\hat{\phi}_{yl}} \\ \vdots \\ e^{i2(N-1)\hat{\phi}_{yl}} \end{bmatrix} \qquad (64)
\end{aligned}$$

Based on the vectors $\mathbf{e}_l$ and $\mathbf{f}_l$ and their linear phase property, $(\hat{\phi}_{xl}, \hat{\phi}_{yl})$ can be expressed as follows:

$$\hat{\phi}_{xl} = \frac{1}{2N-2}\sum_{j=1}^{N-1} \angle\left(\frac{\mathbf{e}_l[j+1]}{\mathbf{e}_l[j]}\right), \qquad (65)$$

$$\hat{\phi}_{yl} = \frac{1}{2N-2}\sum_{j=1}^{N-1} \angle\left(\frac{\mathbf{f}_l[j+1]}{\mathbf{f}_l[j]}\right). \qquad (66)$$

Based on $\left(\hat{\alpha}, \hat{\beta}, \hat{\phi}_{xl}, \hat{\phi}_{yl}\right)$, r_l can be solved from Eqs. (6) and (8) as follows:

$$\hat{r}_l = \frac{1}{2}\left\{\frac{\pi d^2}{\lambda\hat{\phi}_{xl}}\left(1-\sin^2\hat{\alpha}_l\cos^2\hat{\beta}_l\right) + \frac{\pi d^2}{\lambda\hat{\phi}_{yl}}\left(1-\sin^2\hat{\alpha}_l\sin^2\hat{\beta}_l\right)\right\}, \quad l=1,\ldots,L. \tag{67}$$

In the ideal case, if the lth source is in the near-field, the estimate $\hat{r}_l$ lies in $[\lambda/(2\pi), 2D^2/\lambda]$. Otherwise, if it is in the far-field, the estimate $\hat{r}_l$ approaches to infinite. In fact, there are some estimation error due to finite snapshots and existing noise. For convenience, we set $2D^2/\lambda$ as the range threshold to determine whether the lth source is in the far field or near field.

3.4. Description of the Proposed Algorithm

The proposed algorithm can be described as follows:

Step 1: Construct the cumulant matrix $\mathbf{C}$ using Eqs. (19)–(31). Implement SVD of $\mathbf{C}$ using Eq. (32) and obtain $\{\mathbf{U}_s, \mathbf{U}_n, \mathbf{V}_n\}$;

Step 2: Partition $\mathbf{U_s}$ into $\mathbf{U}_1$ and $\mathbf{U}_2$ using Eq. (36), and obtain $e^{j\hat{\theta}_l}$ and $\mathbf{B}_3(e^{j\hat{\theta}_l})$ using Eqs. (39) and (43);

Step 3: Substitute $e^{j\hat{\theta}_l}$ into $\mathbf{D}_1(e^{j\hat{\theta}_l})$ in (45), and obtain $\mathbf{b}_4(\hat{\gamma}_{x_l})$ from the eigenvector corresponding to the smallest eigenvalue of $\mathbf{D}_1(e^{j\hat{\theta}_l})$. Therefore, $\hat{\alpha}_l$ and $\hat{\beta}_l$ can be obtained from the restored virtual steering vector $\mathbf{b}(\hat{\gamma}_{xl}, \hat{\gamma}_{yl})$ using Eqs. (47)–(51);

Step 4: Substitute the estimates $(\hat{\gamma}_{xl}, \hat{\gamma}_{yl})$ into $\mathbf{A}_1(\gamma_{xl}, \gamma_{yl})$ and obtain $\mathbf{a}_2(\hat{\phi}_{xl}, \hat{\phi}_{yl})$ from the EVD of $\mathbf{D}_2(\hat{\gamma}_{xl}, \hat{\gamma}_{yl})$ using Eqs. (60)–(62). Therefore, $\hat{r}_l$ can be obtained from $\mathbf{a}_2(\hat{\phi}_{xl}, \hat{\phi}_{yl})$ using Eqs. (63)–(67).

4. SIMULATION RESULTS

In this section, we compare the proposed algorithm with the cumulant-based algorithm in Refs. [6, 26] as well as the EM method [25] in two ways, i.e., the computational complexity and estimation accuracy.

4.1. Computational Complexity

Regarding the computational complexity, we consider the major part, namely, multiplications involved in cumulant matrix construction,

Table 1. Computational complexity comparison.

	Cumulant matrix computation	SVD/EVD	Iteratio computation	Total computational complexity
Proposed algorithm	$7\times(4N+1)^2K$	$\frac{4}{3}(4N+1)^3$ $+\frac{8}{3}L(2N+1)^3$		$O\begin{pmatrix}7\times(4N+1)^2K\\ +\frac{4}{3}\times(4N+1)^3\\ +\frac{8}{3}L(2N+1)^3\end{pmatrix}$
Ref. [26]	$350\times(2N+1)^2$	$\frac{200}{3}(2N+1)^2$		$O\begin{pmatrix}350\times(2N+1)^2K\\ +\frac{200}{3}\times(2N+1)^2\end{pmatrix}$
EM [25]			$200L\times(4N+1)^2$ $+10\times(4N+1)^2K$	$O\begin{pmatrix}200L\times(4N+1)^2\\ +10\times(4N+1)^2K\end{pmatrix}$

SVD (or EVD) and the iteration operation, The proposed method constructs one $(4N+1)\times(4N+1)$-dimensional cumulant matrix $\mathbf{C}$ and implements its SVD. In addition, it requires implementing EVD of $(2N+1)\times(2N+1)$-dimensional matrices $\mathbf{D}_1(e^{j\theta})$ and $\mathbf{D}_2(\gamma_x,\gamma_y)$ L times. Therefore, the total computational complexity of the proposed algorithm is $O\left(7\times(4N+1)^2K+\frac{4}{3}\times(4N+1)^3+\frac{8}{3}L(2N+1)^3\right)$. The EM algorithm requires at least 10 iterations to obtain the estimations, in each cycle of which the maximization section requires at least 20 iterations [25]. Thus, it requires $O\left(10\times\left(20L\times(4N+1)^2+(4N+1)^2K\right)\right)$. The method in Ref. [26] construct two $(2N+1)^2\times25$-dimensional cumulant matrices and corresponding SVD, so it requires $O\left(350\times(2N+1)^2K+\frac{200}{3}\times(2N+1)^2\right)$. Therefore, the EM algorithm has much higher computational complexity.

The proposed algorithm and the method in Ref. [26] can obtain the parameter estimations with closed analytic solution. However, the EM algorithm requires iteration process to obtain the estimations [25]. The above-mentioned comparisons are shown in Table 1.

4.2. Estimation Accuracy

Some simulations are conducted to assess the estimation accuracy of the proposed algorithm. We consider a 13-element centrosymmetric cross-array with element spacing $d=\lambda/4$. Two equipower, statistically independent sources modeled as $e^{j\zeta_t}$, where the phases ζ_t are uniformly distributed in the interval $[0,2\pi]$. The received signals were polluted by zero-mean additive white Gaussian noises. For comparison, we simultaneously execute the cumulant-based algorithms

in Refs. [6, 26] and the EM method [25]. In addition, the related CRLB on the variance of the estimated parameters are obtained from the inverse of the Fisher information matrix by averaging 500 computations [47]. The DOA (azimuth and elevation) and range estimations are scaled in units of *degree* and *wavelength,* respectively. And the performances of these algorithms are measured by the estimated root mean-square error (RMSE) of 500 independent Monte Carlo runs.

In the first experiment, the proposed algorithm is used to deal with pure near-filed sources. Two near-field sources are located at $\{\alpha_1 = 20^\circ, \beta_1 = 40^\circ, r_1 = 1.5\lambda\}$ and $\{\alpha_2 = 40^\circ, \beta_2 = 30^\circ, r_2 = 2.5\lambda\}$, respectively. In this case, $\phi_{xl} \neq 0$ and $\phi_{yl} \neq 0$, $l = 1, 2$, so both $\mathbf{B}$ and $\mathbf{A}$ have full column rank (see Eqs. (30) and (15) of this paper for details) and thus the proposed algorithm can be applied into pure near-field source localization problem.

The snapshot number is set equal to 400. When the SNR varies from 0 dB to 20 dB, the RMSE of the elevation, azimuth, and range estimations of the two near-field sources from 500 independent Monte Carlo runs using the method in Ref. [26] and the proposed method are shown in Figs. 2, 3, and 4 for comparison. From Figs. 2, 3, and 4, we can see that the proposed algorithm has higher estimation accuracy than that of Ref. [26], but is slightly lower than the EM algorithm [25]. However, the EM algorithm obtains high estimation accuracy at the expense of high computational complexity resulted from the iteration process. As it is expected, when the SNR increases, the estimated values approach to the true values. From Fig. 4, it can be seen that the RMSE of range estimation of the first source (closer to the array) is much lower than that of the second source for the two algorithms and CRLB.

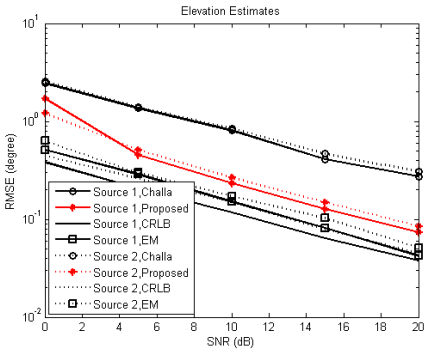

Figure 2. RMSE of elevation estimations versus SNR.

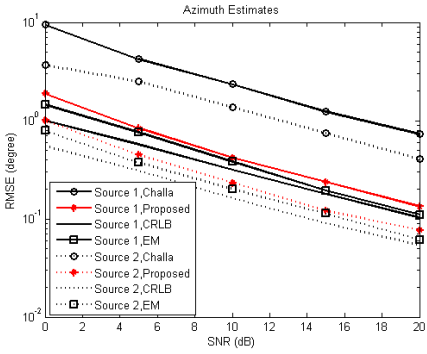

Figure 3. RMSE of azimuth estimations versus SNR.

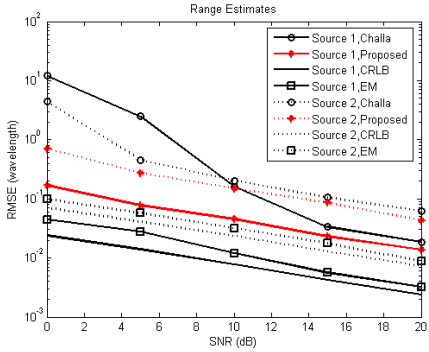

Figure 4. RMSE of range estimations versus SNR.

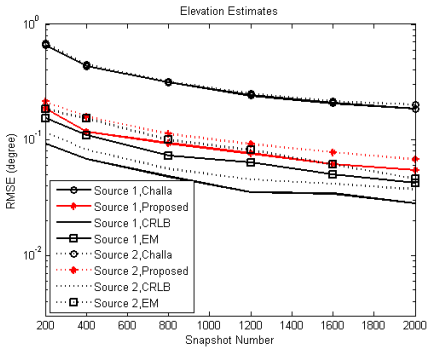

Figure 5. RMSE of elevation estimations versus snapshot number.

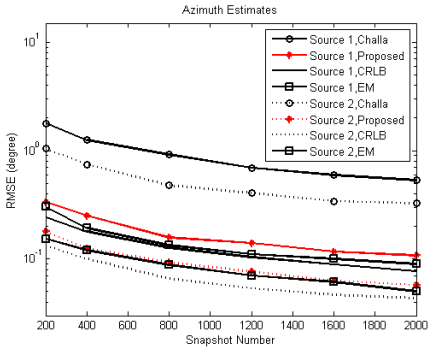

Figure 6. RMSE of azimuth estimations versus snapshot number.

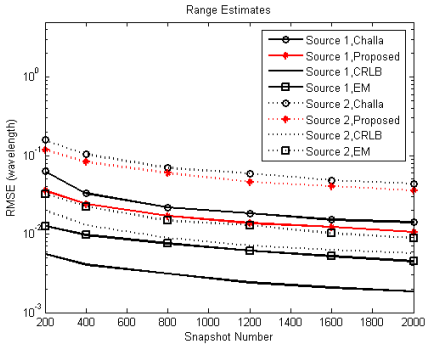

Figure 7. RMSE of range estimations versus snapshot number.

The SNR is fixed at 15 dB. When snapshot number varies from 200 to 2000, the averaged performances (RMSE of elevation, azimuth, and range estimations versus snapshot number for two sources) over 500 Monte Carlo runs are shown in Figs. 5, 6, and 7. From these figures, it can be seen that RMSE of the elevation, azimuth, and range estimations decrease as snapshot number increases. In addition, it can be seen that the proposed algorithm improves estimation accuracy than that of Ref. [26], and approaches the CRLB and the performance of the EM algorithm [25].

In the second experiment, the proposed algorithm is used to deal with one near-filed and one far-field sources. The near-field source is located at $\{\alpha_1 = 20°, \beta_1 = 40°, r_1 = 1.5\lambda\}$; whereas the far-field

source is localized at $\{\alpha_2 = 40^\circ, \beta_2 = 30^\circ, r_2 = \infty\}$. In this case, $\phi_{x1} \neq 0$, $\phi_{y1} \neq 0$, $\phi_{x2} = 0$, and $\phi_{y2} = 0$, so both $\mathbf{B}$ and $\mathbf{A}$ still have full column rank and the proposed algorithm can be applied into one far-field and one near-field source localization problem. The ESPRIT algorithm proposed by Liu and Mendel [6] can localize only the second source (i.e., far-field source). In the method of Ref. [26], $\phi_{x2} = 0$ but $\tan(\gamma_{x2}) + i\tan(\phi_{x2}) \neq 0$. Therefore, the algorithm in [26] can be applied into one far-field and one near-field source localization problem.

The snapshot number is fixed at 400. When the SNR varies from 0 dB to 20 dB, the RMSE of elevation, azimuth, and range (which is only for near-field source) estimations of one near-field and one far-field sources from 500 independent Monte Carlo runs using the two methods are shown in Figs. 8, 9, and 10, respectively. From Figs. 8, 9, and 10, it can be seen that the proposed algorithm has higher estimation accuracy than that of Ref. [26], but slightly lower than the CRLB and the EM algorithm [25].

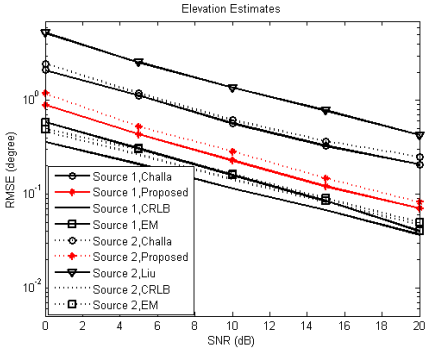

Figure 8. RMSE of range estimations versus snapshot number.

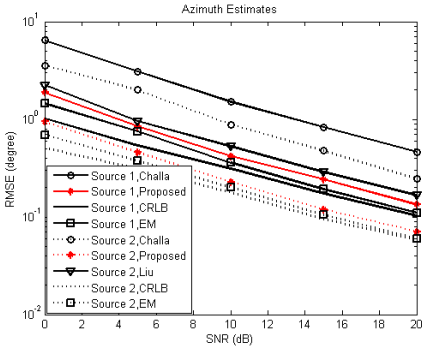

Figure 9. RMSE of azimuth estimations versus SNR.

In the third experiment, the proposed algorithm is used to deal with pure far-field sources. Two far-field sources are localized at $\{\alpha_1 = 20^\circ, \beta_1 = 40^\circ, r_1 = \infty\}$ and $\{\alpha_2 = 40^\circ, \beta_2 = 30^\circ, r_2 = \infty\}$, respectively. In this case, although $\phi_{xl} = 0$ and $\phi_{yl} = 0$, $l = 1, 2$, both $\mathbf{B}$ and $\mathbf{A}$ still have full column rank and the proposed algorithm can be applied into pure far-field source localization problem. The ESPRIT algorithm proposed by Liu and Mendel [6] is suitable for pure far-field sources. In the method of Ref. [26], $\phi_{x1} = 0$ and $\phi_{x2} = 0$ but $\tan(\gamma_{x1}) + i\tan(\phi_{x1}) \neq 0$ and $\tan(\gamma_{x2}) + i\tan(\phi_{x2}) \neq 0$. Therefore, the algorithm in Ref. [26] can be applied into two far-field source localization problem.

The snapshot number is fixed at 400. When the SNR varies from

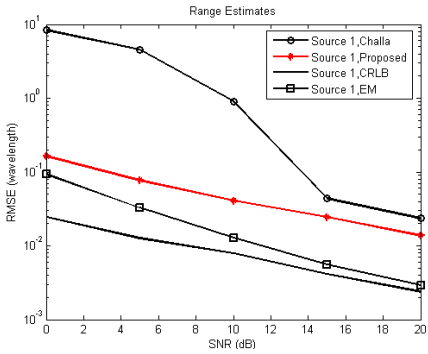

Figure 10. RMSE of range estimates versus SNR.

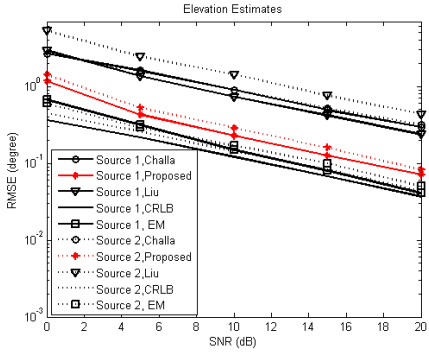

Figure 11. RMSE of elevation estimations versus SNR.

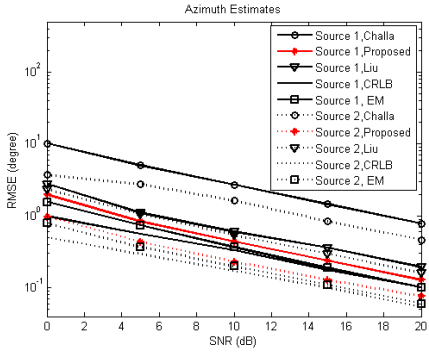

Figure 12. RMSE of azimuth estimations versus SNR.

0 dB to 20 dB, the RMSE of the elevation and azimuth estimations of two far-field sources from 500 independent Monte Carlo runs using the proposed method and CRLB are shown in Figs. 11 and 12, respectively. From Figs. 11 and 12, it can be seen that proposed algorithm has high estimation accuracy.

From the above experiments, we can see that the proposed algorithm with high estimation accuracy can deal with "any-field" sources, i.e., the total received signals by an array consists of either multiple near-field signals, or multiple far-field signals, or their mixture. The method proposed in Ref. [6] can be only applied to pure far-field source localization, and fails in localizing near-field sources. The Unitary ESPRIT algorithm developed in [26] combines two real matrices yields the complex-valued EVD with complex eigenvalues $\tan(\gamma_{xl}) + i\tan(\phi_{xl})$. Even if the l-th source is far-field one, $\phi_{xl} = 0$ but

$\tan(\gamma_{xl}) + i\tan(\phi_{xl}) \neq 0$ and thus the method in Ref. [26] can localize far-field sources. The method in Ref. [26] has lower estimation accuracy than the proposed algorithm since it used half the array sensors to estimate (γ_{xl}, ϕ_{xl}) or (γ_{yl}, ϕ_{yl}). The EM algorithm obtains high estimation accuracy at the expense of high computational complexity resulted from iteration process, and cannot provide the closed analytic solution.

5. CONCLUSION

This paper constructs a special cumulant matrix by exploiting the multiple degrees of freedom available from fourth-order cumulants. Based on its left and right singular vectors, a two-stage separated steering vector-based algorithm is proposed for passive localization of "arbitrary"-field sources in the spherical coordinates. In order to avoid the phase ambiguity, the quarter-wavelength constraint on interment spacing is adopted. In addition, the cross array configuration rather than other geometries is required to simplify the quadratic phase of near-field sources. Since the azimuth-elevation arrival-angles and ranges are estimated from the restored steering vectors, the proposed algorithm can avoid any matching operation and spectral search. The experiment results show that the proposed method is an attractive alternative to localize mixed near-field and far-field sources with closed analytic solution.

ACKNOWLEDGMENT

The authors would like to thank the editor and anonymous reviewers for their valuable comments and suggestion. In addition, this work was supported by the National Natural Science Foundations of China under Grant 60901059 and 61075044, by China Postdoctoral Science Foundation funded project under Grant 201003679 and 20100481355, by the Educational Department Foundation Grant 09JK629 and Natural Science Foundation under 2010JQ8001 of Shaanxi Province, and by the Discipline Union Fund under Grant 116-210905 of Xi'an University of Technology, and the Fundamental Research Funds for the Central Universities of China Grant ZXH2010D012.

REFERENCES

1. Krim, H. and M. Viberg, "Two decades of array signal processing research: The parametric approach," *IEEE Signal Processing Magazine*, Vol. 13, No. 4, 67–94, 1996.

2. Johnson, R. C., *Antenna Engineering Handbook*, 3rd Edition, 9–12, McGraw-Hill, Inc., 2006.
3. Ziomek, L. J., *Fundamentals of Acoustic Field Theory and Space-time Signal Processing*, 410–412, 532–534, CRC Press, Bocaraton, FL, 1995.
4. Schmidt, R., "Multiple emitter location and signal parameter estimation," *IEEE Trans. Antennas and Propagation*, Vol. 34, No. 3, 276–280, 1986.
5. Roy, R. and T. Kailath, "ESPRIT-estimation of signal parameters via rotational invariance techniques," *IEEE Trans. Acoustics, Speech, and Signal Processing*, Vol. 37, No. 7, 984–995, 1989.
6. Liu, T. H. and J. M. Mendel, "Azimuth and elevation direction finding using arbitrary array geometries," *IEEE Trans. Signal Processing*, Vol. 46, No. 7, 2061–2065, Jul. 1998.
7. Tayem, N. and H. M. Kwon, "L-shape 2-dimensional arrival angle estimation with propagator method," *IEEE Trans. Antennas and Propagation*, Vol. 53, No. 5, 1622–1630, May 2005.
8. Veen, A., P. Ober, and E. Deprettere, "Azimuth and elevation computation in high resolution DOA estimation," *IEEE Trans. Acoust. Speech, Signal Processing*, Vol. 40, No. 7, 1828–1832, Jul. 1992.
9. Swindlehurst, A. and T. Kailath, "Azimuth/elevation direction finding using regular array geometries," *IEEE Trans. Aerosp. Electron. Syst.*, Vol. 29, No. 1, 145–156, Jan. 1993.
10. Kedia, Y. S. and B. Chandna, "A new algorithm for 2-D DOA algorithm," *Signal Processing,* Vol. 60, No. 3, 325–332, Mar. 1997.
11. Swindelehurst, A. L. and T. Kailath, "Passive direction-of-arrival and range estimation for near-field sources," *Fourth Annual ASSP Workshop on Spectrum Estimation and Modeling*, 123–128, Minneapolis, Minnesota, USA, Aug. 1988.
12. Cekli, E. and H. A. Cirpan, "Unconditional maximum likelihood approach for near-field source localization," *International Journal of Electronics and Communications*, Vol. 57, No. 1, 9–15, 2003.
13. Grosicki, E., K. Abed-Meraim, and Y. Hua, "A weighted linear prediction method for near-field source localization," *IEEE Trans. Signal Processing*, Vol. 53, No. 10, Part 1, 3651–3660, 2005.
14. Abed-Meraim, K., Y. Hua, and A. Belouchrani, "Second-order near-field source localization: Algorithm and performance analysis," *The Thirtieth Asilomar Conference on Signals, Systems & Computers*, Vol. 1, 723–727, Pacific Grove, California, USA, Nov. 1997.

15. Gorosicki, E. and K. Abed-Meraim, "A weighted linear prediction method for near-field source localization," *Proceedings of the IEEE International Conference on Acoustics, Speech, and Signal Processing*, Vol. 3, 2957–2960, May 2002.
16. Huang, Y. D. and M. Barkat, "Near-field multiple source localization by passive sensor array," *IEEE Trans. Antennas and Propagation*, Vol. 39, No. 7, 968–975, 1991.
17. Jeffers, R., K. L. Bell, and H. L. van Trees, "Broadband passive range estimation using MUSIC," *Proceedings of the IEEE International Conference on Acoustics, Speech, and Signal Processing*, Vol. 3, 2921–2924, May 2002.
18. Weiss, A. J. and B. Friedlander, "Range and bearing estimation using polynomial rooting," *IEEE Journal of Oceanic Engineering*, Vol. 18, No. 4, 130–137, 1993.
19. Starer, D. and A. Nehorai, "Passive localization of near-field sources by path following," *IEEE Trans. Signal Processing*, Vol. 42, No. 3, 677–680, 1994.
20. Challa, R. N. and S. Shamsunder, "High-order subspace based algorithms for passive localization of near-field sources," *The Twenty-ninth Asilomar Conference on Signals, Systems & Computers*, Vol. 2, 777–781, Pacific Grove, California, USA, Oct. 1995.
21. Yuen, N. and B. Friedlander, "Performance analysis of higher order ESPRIT for localization of near-field sources," *IEEE Trans. Signal Processing*, Vol. 46, No. 3, 709–719, 1998.
22. Lee, J. H. and C. H. Tung, "Estimating the bearings of near-field cyclostationary signals," *IEEE Trans. Signal Processing*, Vol. 50, No. 1, 110–118, Jan. 2002.
23. Lee, J. H., Y. M. Chen, and C. C. Yeh, "A covariance approximation method for near-field direction finding using a uniform linear array," *IEEE Trans. Signal Processing*, Vol. 43, No. 5, 1293–1298, May 1995.
24. Liang, J. and D. Liu, "Passive localization of near-field sources using cumulant," *IEEE Sensors Journal*, Vol. 9, No. 8, 953–960, Aug. 2009.
25. Kabaoglu, N., H. A. Cirpan, E. Cekli, and S. Paker, "Deterministic Maximum likelihood Approach for 3-D near-field source localization," *International Journal of Electronics and Communications*. Vol. 57, No. 5, 345–350, 2003.
26. Challa, R. N. and S. Shamsunder, "Passive near-field localization of multiple non-Gaussian sources in 3-D using cumulant," *Signal*

Processing, Vol. 65, 39–53, 1998.

27. Liang, J., S. Yang, J. Zhang, L. Gao, and F. Zhao, "4D near-field source localization using cumulant," *EURASIP Journal on Applied Signal Processing*, Vol. 2007, 1–10, 2007, Doi:10.1155/2007/17820.
28. Yang, D., J. Shi, and B. Liu, "A new near-field source localization algorithm based on generalized ESPRIT," *The 4th IEEE conference on Industrial Electronics and Applications*, 1115–1120, Xi'an, China, Jun. 2009.
29. Abed-Meraim, K. and Y. Hua, "3-D near field source localization using second order statistics," *The Thirty-first Asilomar Conference on Signals, Systems & Computers*, Vol. 2, 1307–1311, Pacific Grove, California, USA, Nov. 1997.
30. Ikram, M. Z., K. Abed-Meraim, and Y. Hua, "Fast quadratic phase transform for estimating the parameters of multicomponent chirp signals," *Digital Signal Processing*, 127–135, Jul. 1997.
31. Ward, D. B. and G. W. Elko, "Mixed near field/far field beamforming: A new technique for speech acquisition in a reverberant environment," *IEEE Workshop on Applications of Signal Processing to Audio and Acoustics*, 19–22, New Paltz, NY, 1997.
32. Agrawah, M., R. Abrahamsson, and P. Ahgren, "Optimum beamforming for a nearfield source in signal correlated interferences," *Signal Processing*, Vol. 86, No. 5, 915–923, 2006.
33. Doclo, S. and M. Moonen, "Design of far-field and near-field broadband beamformers using eigenfilters," *Signal Processing*, Vol. 83, No. 12, 2641–2673, 2003.
34. Arslan, G., F. A. Sakarya, and B. L. Evans, "Speaker localization for far-field and near-field wideband sources using neural networks," *IEEE Workshop on Nonlinear Signal and Image Processing*, Antalya, Turkey, Vol. 2, 528–532, 1999.
35. Argentieri, S., P. Danes, and P. Soueres, "Modal analysis based beamforming for nearfield or farfield speaker localization in robotics," *Proceedings of the 2006 IEEE International Conference on Robots and Systems*, 866–871, 2006.
36. Mukai, R., H. Sawada, S. Araki, and S. Makino, "Frequency-domain blind source separation of many speech signals using near-field and far-field models," *EURASIP Journal on Applied Signal Processing*, Vol. 2006, 1–13, 2006.
37. Kennedy, R. A., D. B. Ward, P. Thushara, and D. Abhayapala, "Nearfield beamforming using nearfield/farfield reciprocity,"

Proceedings of the IEEE International Conference on Acoustics, Speech, and Signal Processing, Vol. 5, 3741–3744, Munich, 1999.

38. Liang, J., X. Zeng, B. Ji, et al., "A computational efficient algorithm for joint range-DOA-frequency estimation of near-field sources," *Digital Signal Processing*, Vol. 19, No. 4, 596–611, 2009.
39. Liang, J. and D. Liu, "Passive localization of near-field sources using cumulant," *IEEE Sensors Journal*, Vol. 9, No. 8, 953–960, Aug. 2009.
40. Dogan, M. C. and J. M. Mendel, "Applications of cumulants to array processing — Part I: Aperture extension and array calibration," *IEEE Trans. Signal Processing*, Vol. 43, No. 5, 1200–1216, May 1995.
41. Porat, B. and B. Friedlander, "Direction finding algorithms based on higher order statistics," *IEEE Trans. Signal Processing*, Vol. 39, No. 9, 2016–2024, Sep. 1999.
42. Chevalier, P., L. Albera, and P. Comon, "On the virtual array concept for higher order array processing," *IEEE Trans. Signal Processing*, Vol. 53, No. 4, 1254–1271, Apr. 2005.
43. Chevalier, P. and A. Ferreol, "On the virtual array concept for the fourth-order direction finding problem," *IEEE Trans. Signal Processing*, Vol. 47, No. 5, 2592–2595, May 1999.
44. Liang, J. and D. Liu, "Joint elevation and azimuth direction finding using L-shaped array," *IEEE Trans. Antennas and Propagation*, Vol. 58, No. 6, 2136–2141, 2010.
45. Gao, F. and A. B. Gershman, "A generalized ESPRIT approach to direction-of-arrival estimation," *IEEE Signal Processing Letters*, Vol. 12, No. 3, 254–257, 2005.
46. Barabell, A. J., "Improving the resolution performance of eigenstructure-based direction-finding algorithms," *Proceedings of the IEEE International Conference on Acoustics, Speech, and Signal Processing*, 336–339, Boston, MA, May 1983.
47. Kay, S. M., *Fundamentals of Statistical Signal Processing: Estimation Theory*, Prentice Hall, Upper Saddle River, NJ, 1993.